ELECTRON BEAM ADDITIVE MANUFACTURING OF Ni-Ti ALLOY

[1]Marek Stanisław WĘGLOWSKI, [1]Sylwester BŁACHA, [1]Krzysztof KWIECIŃSKI, [1]Piotr ŚLIWIŃSKI, [2]Jan DUTKIEWICZ, [2]Łukasz ROGAL

[1]*Łukasiewicz – Institute of Welding, Gliwice, Poland, EU, marek.weglowski@is.gliwice.pl, sylwester.blacha@is.gliwice.pl, krzysztof.kwiecinski@is.gliwice.pl, piotr.sliwinski@is.gliwice.pl*

[2]*Institute of Metallurgy and Materials Science PAS, Krakow, Poland, EU, j.dutkiewicz@imim.pl, l.rogal@imim.pl*

https://doi.org/10.37904/metal.2020.3619

Abstract

Shape memory alloys (such as Ni-Ti) are a unique class of active materials, which can recover to their original shape after applying stimuli, such as deformation due to stress, heat or magnetic field. These alloys possess attractive characteristics such as ability to provide large recoverable strain during mechanical loading (pseudoelasticity), shape recovery upon heating (shape memory effect), and potent biocompatibility, which make alloys one of the suitable actuators for biomedical applications. In the present paper the results of microstructure, martensitic transformation behaviour and superelastic properties of Ni-Ti alloys fabricated using a EBAM technique, which applies wire as the additive material were presented. It was revealed that the microstructure of the deposit exhibited typical solidification features of columnar grains of austenite, due to epitaxial growth mechanism. Moreover, EBSD investigations revealed that the preferential grain orientation in [001] is a result of the adopted material layer deposition. TEM studies have shown presence of martensitic needles partially twinned within austenitic matrix, and a low dislocation density within austenite confirming ability of the EBAM manufactured sample to pseudoelastic deformation at room temperature.

Keywords: Electron beam additive manufacturing, shape memory alloys, microstructure, martensitic transformation

1. INTRODUCTION

As regards welding technologies, three groups of methods can be used for the additive manufacturing (AM) of metallic elements. The three aforementioned technologies utilise the following sources of heat: welding electric arc (WAAM – wire arc additive manufacturing), laser beam (WLAM – wire laser additive manufacturing) and finally electron beam (EBAM – electron beam additive manufacturing). The thickness of a single layer and the rate of deposition in the wire-based AM are significantly greater in comparison with powder-based prototyping methods. The dimensional accuracy of elements made using a wire is lower than that of products made using powder-based technologies. In addition, the surface roughness (corrugation) of the final part is higher. In turn, methods involving the deposition of a wire provide higher process efficiency. The most commonly used AM methods involving the use of a wire and welding electric arc include TIG, MIG/MAG and plasma arc. Laser wire AM can be performed using both CO_2 lasers and solid-state lasers [1, 2]. However, it should be noted, that the AM components may be structurally different from those manufactured from the workpieces obtained via commonly used processes such as casting, rolling, forging, etc. In connection with this, there is a necessity of characterizing them for structural, physico-mechanical and chemical properties.

A concentrated electron beam is characterized by more than 90% energy efficiency which makes it an attractive source of energy for the production of components with AM technologies. Studies carried out so far [3] have shown that AM technologies using wire and electron beam can be used, among others in various missions carried out in space. However, Tarasov et al. [4] have shown that the heat input level in electron beam wire-feed AM proved is an effective process parameter for controlling the amount of δ-ferrite in stainless steels, forming a crystallographic texture and thus controlling corrosion resistance. Wanjara et al. [5] have shown that the use of EBAM process with wire of Ti-6Al-4V alloy allows to achieve bulk microhardness in the deposit of 319 HV and 304 HV in the as-deposited and stress relieved conditions, respectively, which was statistically comparable to the parent material hardness of 322 HV and 314 HV in the as-received and stress relieved conditions, respectively. Moreover, the static tensile properties (914 MPa) of the Ti6Al4V EBAM met adequately the minimum requirements of the standards of cast Ti6Al4V. Manjunath et. al. [6] describes the benefits of using the Taguchi method to analysis the effect of weld parameters on additively deposited layer width during the EBAM process of Ti6Al4V alloy. Confirmation tests are carried out after obtaining optimized parameters and results are correlated with obtained results. The EBAM supplies a very efficient, high power energy source, which easily couples with metals promising one of the highest deposition rates for all metal AM technologies. Simultaneously, the processing in high vacuum is ideal for reactive alloys such as titanium alloys. Thus, EBAM achieves increasingly more acceptance for purpose of industrial applications [7].

On the other hand, the increasing demand for lighter, stronger and functional materials spawned active materials. Shape memory alloys such as nitinol (Nickel Titanium Naval Ordinance Laboratory) has found numerous applications in the medical field including neurology, orthopaedics, interventional radiology and cardiology [8]. Nitinol was discovered [9] in 1959 by Buehler W.J. of the Naval Ordinance Laboratory while trying to develop an impact-, fatigue- and heat-resistant alloy to use as the nose cone of a navy missile. Fatigue and kink resistance, good damping properties and superelasticity have ensured an increased application of nitiniol alloy in surgical applications. Another major factor involves its biocompatibility with research showing it to have similar or better biocompatibility than stainless steel or Ti6Al4V [10]. However, the Young modulus of Ni-Ti alloys (about 50 GPa) is slightly higher than that of a human bone (10-20 GPa), which can result in stress concentration at the connection of the implant with the bone [11].

Simultaneously, it should be noted that due to the extreme small melt pool during AM process, followed by extreme fast cooling but in a next layer followed by partial remelting and reheating, uncommon microstructures are obtained. Those microstructures control the mechanical properties such as strength, ductility, toughness and high residual stresses and, in case of shape memory alloys, also the quality of the functional properties. Moreover, important points of attention for acceptance of a printed product are the density (porosity) and the presence of cracks. A final point of attention is the environment in the production room. In case of laser AM, an argon flow is applied to avoid oxidation. However, complete oxygen-free flow is almost impossible. In this respect, electron beam AM has the advantage that a vacuum environment is applied during processing [12]. Guimarães et. al. [13] that EBAM process is a feasible technology for the 3 printing of NiTi part. They revealed that the as-fabricated material is superelastic at room temperature due to 1) the predominance of the B2 austenitic phase and 2) austenitic final temperature (A_f) of 20 °C. In addition, the phase transformations observed indicates that EBAM keeps the functional properties of NiTi wire base material.

The paper presents the EBAM process of Ni-Ti alloy in relation to microstructure and mechanical properties. The 58 wt% Ni, 0.22 wt% C and Ti – balance alloys showing room temperature pseudoelasticity will be used in the investigation. The importance of this research is to create a scientific basis for adapting the EBAM to produce AM part with shape memory alloy.

2. EXPERIMENTAL PROCEDURE

The wire 1 mm in diameter (50.97 at% Ni, max. 0.22 at% C, Ti balance), delivered by SMATEC company, Belgium, was used for EBAM process. The wire was delivered after heat treatment to modify transformation temperatures. The composition of the sheet substrate delivered also by SMATEC Company, was 50.74 at% Ni, max 0.12 at% C, 0.11 at% O, Ti balance. The different chemical composition of wire and substrate is negligible.

The AM process was conducted using a 30 kW CVE EBAM and welding machine at the Łukasiewicz - Institute of Welding (**Figure 1a**) that comprises an electron beam gun with an accelerating voltage of 150 kV, a wire feeding system and positioning mechanisms that are all housed within a chamber, roughly 1.5 m × 1.5 m × 2.2 m. The system was operated in a vacuum environment with a pressure lower than 2×10^{-3} Pa, wire feedstock, fed from a spool through the wire-feed system, was directed axially into the focal point of the electron beam located on the deposited surface. Both the electron beam gun and wire feeding system were mounted onto an overhead positioning gantry, the substrate was clamped onto a CNC work-table. Operating the EBAM system with real-time computer control, the process parameters, including the voltage, current, wire-feed rate and translation in the X and Z directions were programmed to deposit the NiTi wire as a single bead onto the NiTi substrate so as to build layer by layer a straight wall to target dimensions of 5×10×45 mm (**Figure 1b**).Based on preliminary studies the set of following parameters was applied during the fabrication process: accelerating voltage 60 kV, beam current 15 mA, feeding angle 30°, wire feed speed 1000 mm/min and travelling speed 2000 mm/min.

The microstructural observations of fabricated samples were conducted using a scanning electron microscope (SEM) FEI Versa 3D and a Leica DMIRM optical microscope, on previously etched samples using a Kroll's reagent. EBSD analysis was performed with EDAX Hikari CCD-based detector and a TSL OIM Data collection software version 7.0. The detailed microstructural studies were performed using a transmission electron microscope (TEM) Tecnai FEG G2 F20 Super Twin, equipped with an integrated EDAX Apollo XP energy dispersive X-ray spectrometer (EDS). The thin foils for TEM observations were prepared by electropolishing 100 μm thick discs in an electrolyte containing 10 mol% $HClO_4$ in methanol (voltage 20 V, temperature -20 °C). The compression tests were performed at a Shimadzu Autograph AG-X plus testing machine at strain rate 10^{-3} s^{-1}. The samples for mechanical tests, in the form of cylinders with the diameter of 4 mm and the height of 6 mm, were prepared using an electrical discharge machine. The Differential Scanning Calorimetry (DSC, Q1000 TA Instruments) method was used in order to determine the temperatures of phase transformations. The applied heating/cooling rate was 20 °C/min.

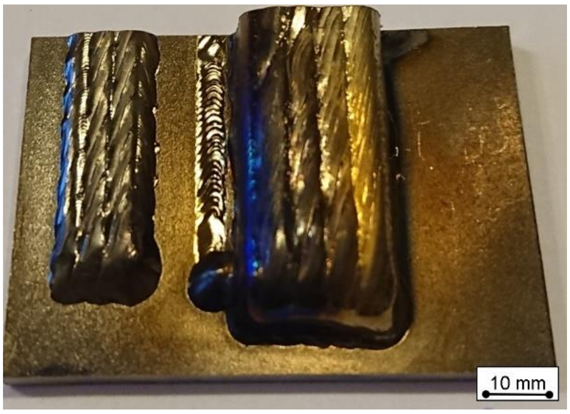

a) b)

Figure 1 a) general view of chamber of XW150:30/756 EBAM machine, b) EBAM part of NiTi alloy

3. RESULTS AND DISCUSSION

Figure 2 shows light micrographs of the microstructure of NiTi elements manufactured using EBAM method. The EBAM allows to manufacture the final part from NiTi shape memory alloy without any defect such as cracks or porosity. The stability of the EBAM process was assured. The microstructures of the interface between the deposited material and the substrate were analysed. The elongated grains, perpendicular to the surface of substrate were observed. Their morphology indicates that, an epitaxial grain growth in the building direction takes place during the deposition [12]. It is typical of the AM process that the penetration depth of an electron beam is larger than the thickness of the deposited layer, therefore part of the beam energy is used to re-melt the surface layer of the element. Due to a high thermal gradient in the created melt pool, conditions for the epitaxial growth of the columnar layer appear at the bottom of the pool. The EBSD analysis was conducted in order to determine the crystallographic texture, grain size of the deposited elements and the orientation dependence between the grains in the substrate and the deposited layers.

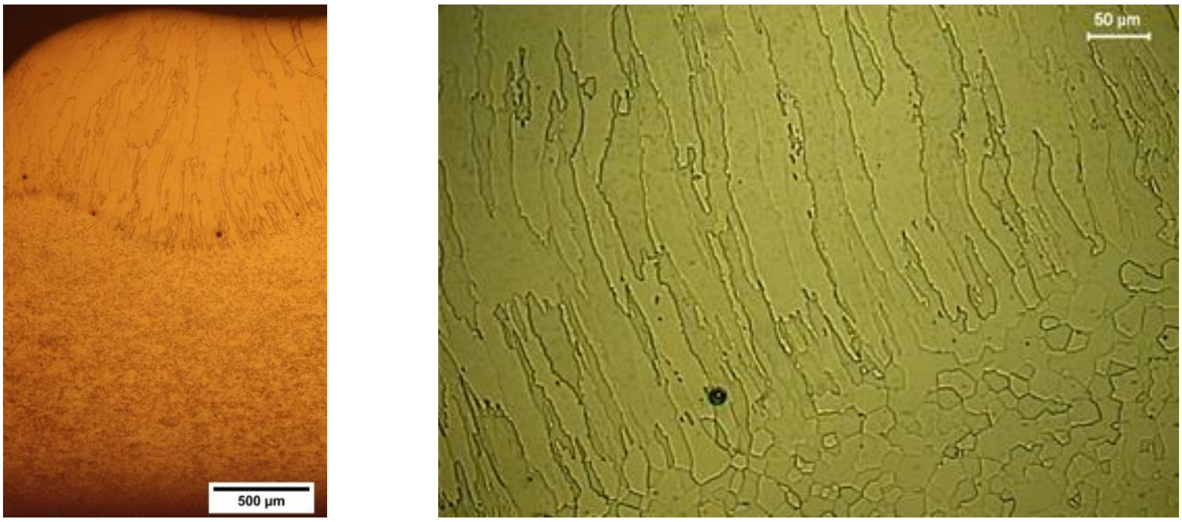

a) b)

Figure 2 Light microscope micrograph of cross section of EBAM deposited sample in the plane parallel to the growth direction, a) general view, b) higher magnification

Figure 3a shows SEM micrograph of EBAM deposited sample. At the grain boundary misorientation map a red lines misorientation respond to 2-5°, green line 5-15°, and blue >15°, respectively. A **Figure 3b** shows grains with colours marked according to the inverse pole figure (IPF) coded map. The IPF maps of NiTi fabricated using the EBAM method, taken of the area just above the interface between the substrate and deposited layers. It should be noted that, the width of the columnar grain is controlled by the size of the equiaxed grains in the substrate near 100 μm. The results confirmed that during the deposition process, the epitaxial crystallization of columnar grains, proceeds in the heat flux direction. **Figure 4a** shows the texture measured on a plane parallel to the direction of growth of the lateral plane is similar to the direction [001] of the beta phase. Visible increase of beta phase orientation in a direction close to [100]. A small deviation from ideal orientation is related to movement during EB deposition process. **Figure 4b** shows a TEM micrograph of the sample deposited on the NiTi substrate using EBAM method with the interface between the B2 austenite and B19' martensite. TEM microstructure from deposited rectangular shape NiTi by EBAM method and SADP (Selected Area Electron Diffraction Pattern) from the central martensitic needle of [001] zone axis orientation showing small number of twins, and a low dislocation density within the austenite. The dislocation density in the case of the material fabricated using EBAM method was much lower in comparison with the samples obtained by LENS technique [14], most probably due to higher energy used and thicker samples causing lower cooling rate, therefore the contribution of that factor to the martensitic transformation temperatures was lower.

The analysis of DSC curves of the EBAM deposited material in the as-deposited and aged states revealed that for the sample in the as-deposited state, a broad diffuse peak is observed, with maximum at -19.2 °C, which is a result of non-homogeneity of the deposited sample with respect to the chemical composition, as well as the grain size. Aging at 500°C for 2h caused the shift of the temperatures of martensitic and reverse transformations towards higher temperatures – M_p from -19.2 °C to -15.4 °C and A_p from 12.2 °C to 31.7 °C, but those changes were not as high as in the LENS deposited material [14]. However, similarly as reported in [13] a small pseudoelastic effect near 3% was observed at room temperature.

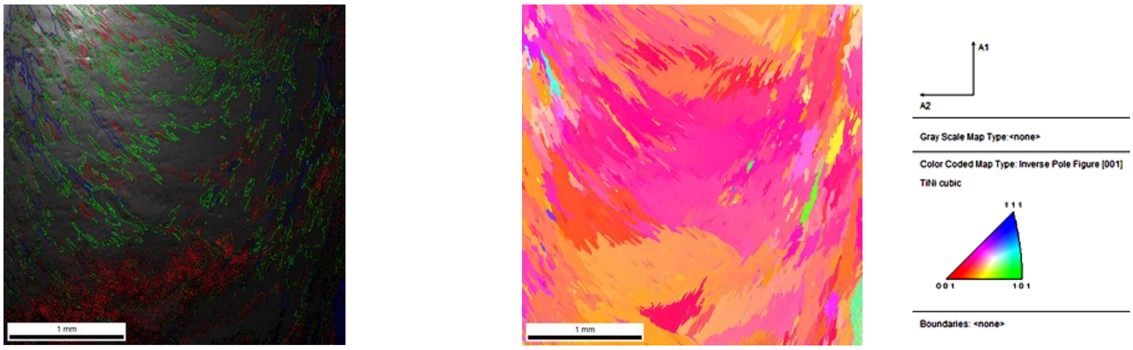

a) b)

Figure 3 SEM micrograph of EBAM deposited sample, a) grain boundary misorientation map; red lines misorientation 2-5°, green 5-15°, blue >15° b) grains with colours marked according to inverse pole figure coded map

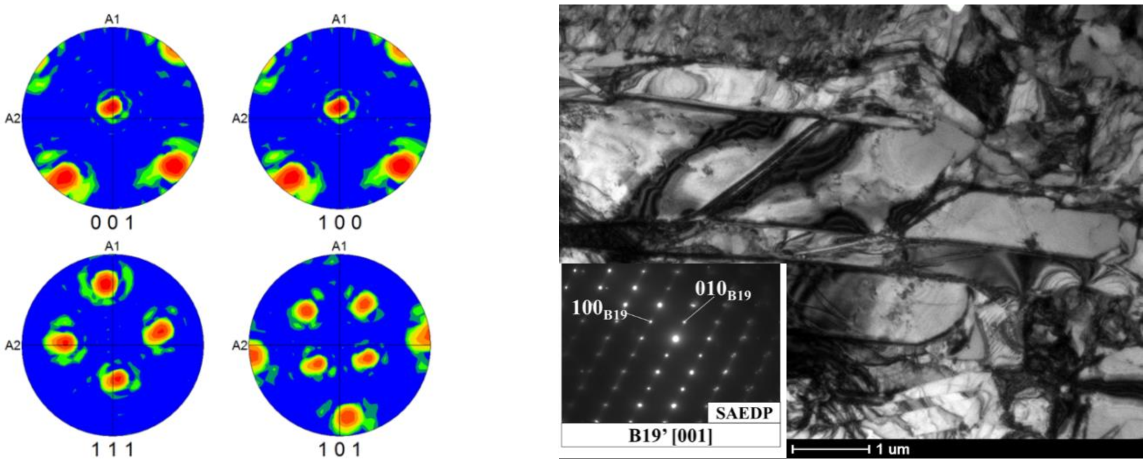

a) b)

Figure 4 a) Inverse pole figure map of NiTi fabricated using EBAM technique, texture measured on a plane parallel to the build direction, b) TEM microstructure and electron diffraction pattern of EBAM deposited sample

4. CONCLUSION

Based on the results of the present research on developing a EBAM with wire feeding of a NiTi shape memory alloy, the following conclusions can be drawn:

- the process of additive manufacturing using an electron beam with filler material in the form of solid wire enables the fabrication of test components with strictly defined technological parameters without any defects,
- the microstructure of the deposit exhibited typical solidification features of columnar grains of austenite, due to epitaxial growth mechanism, resulting from heat transfer direction. EBSD investigations revealed that the preferential grain orientation in [001] is a result of the adopted material layer deposition,
- TEM studies from deposited rectangular shape NiTi alloy by EBAM method have shown presence of martensitic needles partially twinned within austenitic matrix, and a low dislocation density within austenite confirming ability of the EBAM manufactured sample to pseudoelastic deformation at room temperature.

ACKNOWLEDGEMENTS

This work has been performed with funding from National Science Centre in Poland within the frame of the research grant UMO-2016/23/B/ST8/00754 entitled: "Multiscale analysis of physico-chemical processes during rapid prototyping using concentrated energy sources in view of formation of microstructure and mechanical properties".

REFERENCES

[1] WĘGLOWSKI, M.ST., BŁACHA, S., JACHYM, R., DWORAK, J., RYKAŁA, J. Additive Manufacturing with wire – comparison of processes. *AIP Conference Proceedings.* 2113, 150016, 2019, pp. 150016-1-150016-6.

[2] WĘGLOWSKI, M.ST., BŁACHA, S., PILARCZYK, J., DUTKIEWICZ, J., ROGAL, Ł. Electron beam additive manufacturing with wire – Analysis of the process. *AIP Conference Proceedings.* 1960, 140015, 2018, pp. 140015-1-140015-6.

[3] TAMINGER, K.M.B. HARLEY, R.A. DICUS D.L. Solid freeform fabrication: An enabling technology for future space nissions*. Proceedings of International of International Conference on Metal Powder Deposition for Rapid Manufacturing*. San Antonio. 2002, pp. 52-60.

[4] TARASOV, S.YU., FILIPPOV, A.V., SHAMARIN, N.N., FORTUNA, S.V., MAIER, G.G., KOLUBAEV, E.A. Microstructural evolution and chemical corrosion of electron beam wire-feed additively manufactured AISI 304 stainless steel. *Journal of Alloys and Compounds.* 2019, vol. 803, pp. 364-370.

[5] WANJARA, P., WATANABE,K., DE FORMANOIR, C., YANG, Q., BESCOND,C., GODET, S., BROCHU, M., NEZAKI, K., GHOLIPOUR, J., PATNAIK P. Titanium alloy repair with wire-feed electron beam additive manufacturing technology. *Advances in Materials Science and Engineering*. 2019, Article ID 3979471, p. 1-23.

[6] MANJUNATH, A., ANANDAKRISHNAN, V., RAMACHANDRA, S., PARTHIBAN, K., Experimental investigations on the effect of pre-positioned wire electron beam additive manufacturing process parameters on the layer geometry of titanium 6Al4V. *Materials Today: Proceedings*, 2020, vol. 21, pp. 766–772.

[7] BAUFELD, B., WIDDISON, R., DUTILLEU, T. Electron beam additive manufacturing: Deposition strategies and properties. *4th IEBW International Electron Beam Conference*, Aachen, 2017, pp. 114-117.

[8] MWANGI, J.W., NGUYEN, L.T., BUI, V.D., BERGER, T., ZEIDLER, H., SCHUBERT, A. Nitinol manufacturing and micromachining: A review of processes and their suitability in processing medical-grade nitinol. *Journal of Manufacturing Processes*. 2019, vol. 38, pp. 355–369.

[9] KAUFFMAN, G.B., MAYO, I. The story of nitinol: the serendipitous discovery of the memory metal and its applications. *Journal of Chemical Education.* 1997, vol. 2, pp. 1–21.

[10] JANI, J.M., LEARY, M., SUBIC, A., GIBSON, M.A. A review of shape memory alloy research, applications and opportunities. *Materials and Design*. 2014, vol. 56, pp. 1078–1113.

[11] BANSIDDHI, A., SARGEANT, T.D., STUPP S.I., DUNAND, D.C., Porous NiTi for bone implants: a review. *Acta Biomaterialia*. 2008, vol. 4, pp. 773-782.

[12] HUMBEECK J.V. Additive manufacturing of shape memory alloys. *Shape Memory and Superelasticity.* 2018, vol. 4, pp. 309–312.

[13] GUIMARÃES, R.P.M., PIXNER, F., TRIMMEL, G., AMANCIO-FILHO, S.T. 4-D printing of NiTi shape memory alloys. *Advanced Materials Day*, 2019 - TU Graz, poster.

[14] DUTKIEWICZ, J., ROGAL, Ł., KALITA, D., WĘGLOWSKI, M.ST., BŁACHA, S., BERENT, K., CZEPPE, T., ANTOLAK-DUDKA, A., DUREJKO, T., CZUJKO, T. Superelastic effect in NiTi alloys manufactured using electron beam and focused laser rapid manufacturing methods. *Journal of Materials Engineering and Performance.* 2020, Vol. 29, pp. 4463–4473.